https://doi.org/10.5194/cp-2023-6
Preprint. Discussion started: 24 February 2023

Climate of the Past Discussions

Disparate energy sources for slow and fast Dansgaard-Oeschger cycles

Diederik Liebrand[1, 2, 3, *], Anouk T. M. de Bakker[4, *], Heather. J. H. Johnstone[3] & Charlotte S. Miller[3]

[1]Department of Earth and Environmental Sciences, The University of Manchester, Manchester, United Kingdom.
[2]British Ocean Sediment COre Research Facility (BOSCORF), National Oceanography Centre, Southampton, United Kingdom
[3]Center for Marine Environmental Sciences (MARUM), University of Bremen, Klagenfurter Straße 4, 28359 Bremen, Germany.
[4]Unit of Marine and Coastal Systems, Deltares, Boussinesqweg 1, 2629 HV, Delft, the Netherlands.
*These authors contributed equally: Diederik Liebrand, Anouk T. M. de Bakker.

Correspondence to: Diederik Liebrand (diederik.liebrand@manchester.ac.uk) and/or Anouk T. M. de Bakker (anouk.debakker@deltares.nl)

Abstract. During the Late Pleistocene, Dansgaard-Oeschger (DO) cycles triggered warming events that were as abrupt as the present-day human-induced warming. However, in absence of a periodic forcing operating on millennial time scales, the main energy sources of DO cycles remain debated. Here, we identify the energy sources of DO cycles by applying a bispectral analysis to the North Greenland ice core project (NGRIP) oxygen isotope ($\delta^{18}O_{ice}$) record—a 123-thousand-years (kyr) long proxy-record of air-temperatures (T_{air}) over Greenland. For both modes of DO cyclicity—slow and fast—we detect disparate energy sources. Slow-DO cycles are marked by multi-millennial periodicities in the 12.5 to 2.5 kyr bandwidth and receive energy from astronomical periodicities. Fast-DO cycles have millennial periodicities in the 1.5 ± 0.5 kyr range and receive energy from centennial periodicities. We propose cryospheric and oceanic mechanisms that facilitate the transfer of energy from known sources to slow- and fast-DO cycles, respectively. Our findings stress the importance of understanding energy-transfer mechanisms across a broad range of time scales to explain the origins of climate cycles without primary periodic energy-sources.

1 Introduction

Climate variability on (multi-) millennial time scales is an enigmatic phenomenon because there is no consensus about the energy sources for this variability (Braun et al., 2005;Schulz et al., 2002;Wara et al., 2000;Sun et al., 2021;Stuiver and Braziunas, 1993;Zhang et al., 2021). Astronomical climate forcing—a nonlinear response of the Earth's climate system to changes in the distribution of incoming solar radiation (insolation) across the hemispheres/seasons—can explain the variability in palaeoclimate time series in the Milankovitch band (Hays et al., 1976;Liebrand and de Bakker, 2019;Riechers et al., 2022) (i.e., tens to hundreds of thousands of years). Similarly, solar forcing through modest changes in the total annual amount of insolation the Earth receives, resulting from the ~11-year sunspot cycle (±0.15%), can explain palaeoclimate

https://doi.org/10.5194/cp-2023-6
Preprint. Discussion started: 24 February 2023


Climate of the Past Discussions

variability on time scales that range from the annual and decadal, up to the centennial (Peristykh and Damon, 2003;Wagner et al., 2001;Huybers and Curry, 2006;Stuiver and Braziunas, 1993). The presence of energy sources for climate variability on these time scales, starkly contrast with the absence of a widely accepted forcing agent on the in-between millennial and multi-millennial periodicities (Pestiaux et al., 1988;Pelletier, 1998;Hagelberg et al., 1994;Huybers and Curry, 2006;Hagelberg et al., 1991;Braun et al., 2005;Braun et al., 2009;Rousseau et al., 2022;Scafetta et al., 2016) (a thousand to ten thousand years). Insolation has been suggested to vary on these timescales (Scafetta et al., 2016;Kelsey, 2022), but the geological archive cannot be straightforwardly interpreted as a true recorder of (changes in the distribution of) solar output on millennial time scales, due to the many nonlinear response mechanisms of the Earth's climate system. To advance the debate about what "fuels" millennial climate cycles, it is thus essential to see if millennial climate variability is cyclic (Ditlevsen et al., 2005) (i.e., periodic), and if so, where the energy is derived from.

The most notable example of millennial climate variability are the DO cycles observed in the NGRIP $\delta^{18}O_{ice}$ record (Andersen et al., 2004) (from Greenland). As an T_{air} proxy record for the past 123 kyr (Late Pleistocene to Holocene), the NGRIP $\delta^{18}O_{ice}$ chronology is unsurpassed in its resolution, dating precision and accuracy, and detail of structure in the data (i.e., signal-to-noise ratio) (Andersen et al., 2004;Kindler et al., 2014;Vinther et al., 2006;Rasmussen et al., 2006;Andersen et al., 2006;Svensson et al., 2008;Wolff et al., 2010). This level of data quality probably constitutes a permanent ceiling in what can be reconstructed using climate proxies from any of Earth's natural archives, because no marine or terrestrial record will probably ever be able to match ice core chronologies in all these respects simultaneously. A comprehensive statistical analysis of the NGRIP $\delta^{18}O_{ice}$ record—including a higher order spectral analysis—is thus essential if we want to fully probe the climate dynamics across centennial, millennial, and astronomical time scales captured in this unique chronology. Previous statistical tests showed that certain spectral peaks in marine records were lower or higher harmonics of a primary cyclic signal (Hagelberg et al., 1994;Riechers et al., 2022); findings suggestive of frequency- and phase-coupling among climate cycles. However, these analyses were not able to detect direction and magnitude of energy transfers among climate cycles. We overcome the shortcomings of these methods by computing directions and magnitudes of energy transfers among climate cycles in the NGRIP $\delta^{18}O_{ice}$ record directly from the bispectrum—a statistical technique originally developed by the climatologist and 2021 Nobel-laureate in Physics Klaus Hasselmann and colleagues to investigate the nonlinear origins of near-shore ocean waves (Hasselmann et al., 1963). Here we apply an advanced interpretation of the bispectrum (de Bakker et al., 2015;Liebrand and de Bakker, 2019;Herbers et al., 2000) (i.e., the total and zonal integrations of the imaginary part of the bispectrum) to the NGRIP $\delta^{18}O_{ice}$ record and show that both slow and fast DO cycles derive their energy from largely disparate astronomical and centennial sources through nonlinear interactions inherent to the climate-cryosphere system. These findings may abolish the need for invoking millennial forcing agents to explain millennial climate cycles (Scafetta et al., 2016).

https://doi.org/10.5194/cp-2023-6
Preprint. Discussion started: 24 February 2023

Climate of the Past Discussions

2 Asymmetric DO cycles in the NGRIP $\delta^{18}O_{ice}$ record

In total, 26 quasi-periodic DO cycles are currently recognized in the NGRIP $\delta^{18}O_{ice}$ record (see Appendix A), some of which are subdivided into a few shorter lasting episodes (Andersen et al., 2004;Dansgaard et al., 1993;Rasmussen et al., 2014) (Fig. 1a). They are characterized by abrupt warming events at the base of relatively warm interstadials ($\delta^{18}O_{ice}$ = –36 to –40 ‰, $T_{air} \approx$ –35 to –40 ºC), followed by either several stepwise and rapid, or one more gradual, T_{air} decrease(s), which lead(s) to longer-lasting and colder stadials ($\delta^{18}O_{ice}$ = –40 to –45 ‰, $T_{air} \approx$ –50 ºC) (Kindler et al., 2014) (Fig. 1a). For most DO events this evolution—an abrupt warming followed by a stepwise or a more gradual cooling—results in asymmetric (i.e., sawtooth-shaped) cycle shapes (Hagelberg et al., 1991;King, 1996) or waveforms. According to bispectral theory (de Bakker et al., 2015;Herbers et al., 2000), asymmetric cycle shapes in time series constitute a prognostic geometry for the nonlinear transfer of energy across the power spectrum. Outside of Greenland, climate variability highly comparable to the DO cycles in structure is recognized in planktonic foraminiferal $\delta^{18}O$ values from the Iberian Margin. This indicates that sea-surface temperatures in the wider North Atlantic region were as variable on millennial time scales as the T_{air} cycles over Greenland (Shackleton et al., 2000). Evidence for the global climatic expression of Late Pleistocene millennial climate variability, albeit more subdued, comes from, e.g., benthic foraminiferal $\delta^{18}O$ values (i.e., deep water temperatures) from the Iberian Margin (Shackleton et al., 2000), from δD (i.e., air-temperature) and methane records from the Antarctic ice core chronology (Loulergue et al., 2008), and from globally distributed speleothem records (Menviel et al., 2020;Corrick et al., 2020).

Prior to investigating the asymmetric cycle shapes of the NGRIP $\delta^{18}O_{ice}$ record in more detail, we reassess the (quasi-) periodic nature of millennial climate cycles (Alley et al., 2001;Hinnov et al., 2002;Matyasovszky, 2010;Schulz et al., 1999) (Fig. 1c). We note that there is a lack of consensus in the literature about the presence/absence of periodic components in the NGRIP $\delta^{18}O_{ice}$ record, with some studies arguing against any form of periodicity in favour of purely stochastically induced DO "events" (Ditlevsen et al., 2007;Ditlevsen et al., 2005;Kleppin et al., 2015;Gottwald, 2021). However, considering our new bispectral results that identify a clear grouping in the distribution of *nonsinusoidality* (i.e., asymmetry) per frequency (see next paragraph), we believe that also a reassessment of the distribution of *sinusoidality* per periodicity is justified. To do so, we apply a wavelet analysis to the data (Fig. 1c) (see Appendix B). Similar to previous studies that performed spectral analysis on the NGRIP $\delta^{18}O_{ice}$ record (Riechers et al., 2022;Mitsui et al., 2019;Petersen et al., 2013), we identify two distinct modes of DO variability in the time-periodicity domain: (*i*) slow-DO cycles, which are marked by sub-astronomical/multi-millennial periodicities in the 12.5 to 2.5 kyr bandwidth (Dansgaard et al., 1984) (e.g., DO cycles 1, 8, 12, 19, 20, and 22), and (*ii*) fast-DO cycles that have millennial periodicities in the 1.5 ± 0.5 kyr range (Dansgaard et al., 1984;Braun et al., 2005;Ditlevsen et al., 2007;Schulz, 2002;Schulz et al., 1999) that extends into the centennial periodicity range, (e.g., DO cycles 3, 4, 5, 6, 7, 9, 10, 11, and 18) (Fig. 1c). Slow-DO cycles are near-continuously present throughout the record and are especially strongly expressed from 110 to105 thousand years ago (ka), from 80 to 70 ka, from 50 to 35 ka, and from 15 to 10 ka. Slow-DO cycles contribute to the variance associated with the Eemian and Holocene interglacials, as well as high

https://doi.org/10.5194/cp-2023-6
Preprint. Discussion started: 24 February 2023

Climate of the Past Discussions

amplitude DO Cycles 1 (i.e., Bølling–Allerød/Younger Dryas), 19 and 20 (Fig. 1). Fast-DO cycles are briefly present from 110 to 105 ka, and near-continuously expressed from 90 to 10 ka. The distinction in cycle durations between the two modes of DO variability suggests that there may be at least two distinct climatic mechanisms at their root-cause.

3 Energy transfers among climate cycles shed light on the "black box" climate system

To further probe the origins of both slow- and fast-DO cycles in the NGRIP $\delta^{18}O_{ice}$ record, we apply a bispectral analysis (Fig. 2) to the detrended, and Hamming-tapered data (see Appendix B). Bispectral analysis is a statistical technique that can deconvolve the asymmetry (i.e., sawtoothness) of a periodic signal into three parts. These constituents, one sum-frequency (f_3, i.e., $f_3 = f_1 + f_2$) and two difference-frequencies (f_1 and f_2, i.e., $f_1 = f_3 - f_2$, and $f_2 = f_3 - f_1$), can either gain (orange and red colours for f_3, blue colours for f_1 and f_2) or lose (blue colours for f_3, orange and red for f_1 and f_2) energy (Fig. 2, Supp. Figs. S1, S2, Supp. Table S1). This makes bispectral analysis a powerful technique to identify energy sources of asymmetric periodic signals. In the bispectrum of the NGRIP $\delta^{18}O_{ice}$ record (Fig. 2), we observe three slow-DO periodicities that stand out by being involved in many energy exchanges; namely: the 6.1, 4.2, and 3.7 kyr cycles. For fast-DO cycles, we observe more subtle interactions at the crossing lines with the 40 kyr obliquity and 23 kyr precession cycles, and, more prominently, with the 4.2 and 3.7 kyr slow-DO cycles. *Relative* energy transfers among climate cycles, and their directions, can thus be derived from the bispectrum. The bispectrum shows that slow- and fast-DO cycles have highly complex, and mixed energy sources from across a wide range of periodicities. But, the *net* effect per periodicity of all individual energy exchanges cannot be derived from the bispectrum alone because individual periodicities are represented in the bispectrum as f_1, f_2, and f_3 simultaneously, each of which can gain and/or lose energy (de Bakker et al., 2015;Liebrand and de Bakker, 2019) (see Appendix B).

To obtain magnitudes of net energy transfers per periodicity/climate cycle, we need to integrate over the bispectrum (see Appendix B). The total integration of the bispectrum of the NGRIP $\delta^{18}O_{ice}$ record reveals three distinct bandwidths in the periodicity domain, each marked by distinct regimes in energy losses and/or gains (Fig. 3b). First, the astronomical periodicities of ~110 kyr eccentricity, 40 kyr obliquity, and ~20 kyr precession, lose energy. Second, periodicities of slow-DO cycles, covering the bandwidth from 12.5 to 2.5 kyr, predominantly gain net energy. Third, fast-DO cycles and centennial periodicities, in the 2.5 to 0.1 kyr periodicity range, are marked by rapidly alternating net energy gains and losses that seem to largely balance one another across this part of the spectrum. However, an overall loss in energy is observed at periodicities in the range between 0.3 and 0.1 kyr (Fig. 3b). Net energy gains that stand out in amplitude are the slow-DO cycles with periodicities of 6.1, 4.2, and 3.7 kyr, as well as the gains at the 2.9, and 2.7 kyr periodicities. Some further notable net energy gains coincide with the 1.5 ± 0.5 kyr periodicity range of the fast-DO cycles, such as the 1.7, 1.5, and 1.3 kyr periodicities. Other well-expressed gains fall in the centennial bandwidth; being the 0.9, 0.5, 0.4, and 0.2 kyr periodicities. By integrating over the bispectrum we show which periodicities gain and lose energy, and thus how energy is

https://doi.org/10.5194/cp-2023-6
Preprint. Discussion started: 24 February 2023


Climate of the Past Discussions

redistributed over the power spectrum. Based on this new information we can piece together cause-and-effect relationships otherwise unobservable within the "black-box" of Earth's climate system and derive an origin-story for both slow- and fast-DO cycles.

By comparing the power spectrum of insolation (Fig. 3a) to the total integration of the bispectrum (Fig. 3b) and power spectrum (Fig. 3c) of the NGRIP $\delta^{18}O_{ice}$ record, we show that part of the energy the Earth receives on astronomical time scales (Fig. 3a) is lost (Fig. 3b) and transferred toward shorter periodicities, particularly those of slow-DO cycles (Fig. 3b, c). Slow-DO cycles thus have an indirect astronomical origin (Sun et al., 2021), at least in part. Furthermore, we observe several distinct energy gains in the 1.5 ± 0.5 kyr periodicity range of fast-DO cycles, which are accompanied by smaller amplitude energy losses. These net gains show that part of the spectral power associated with fast-DO cycles is derived from nonlinear interactions with other climate cycles (Fig. 3b, c). However, from the total integration of the bispectrum, it is hard to make out whether most of this energy is derived from astronomical or other fast-DO and centennial cycles.

To better identify the separate energy sources for both slow- and fast-DO cycles, we devise a zonation scheme. This zonation scheme aims to isolate groups of nonlinear interactions among specific frequency bandwidths. It consists of nine unique combinations of the three main bandwidths: (*i*) astronomical, (*ii*) slow-, and (*iii*) fast-DO and centennial periodicities (Fig. 2, Supp. Fig. S1, Supp. Table S1). Boundaries for the zonal integration are selected at frequencies where the qualitative behaviour of energy transfers in the total integration changes (see previous paragraph). This results in $f = 80$ Myr^{-1} ($p = 12.5$ kyr) for the boundary between astronomical and slow DO cycles, and at $f = 400$ Myr^{-1} ($p = 2.5$ kyr) for the boundary between slow DO and fast DO cycles. Subsequently, we integrate the bispectrum of the NGRIP $\delta^{18}O_{ice}$ record zonally (de Bakker et al., 2015;Liebrand and de Bakker, 2019) (Fig. 4) (see Appendix B). From the zonal integrations we learn that most energy is exchanged among astronomical and slow-DO cycles (Zone 3, Fig. 4c), which results in a net transfer of energy to the 3.7 kyr cycle. Other energy sources for slow-DO cycle now also become apparent; additional energy is sourced from fast-DO periodicities in the range between 2.0 and 2.5 kyr (Zone 6, Fig. 4f) and broadly from across the millennial to centennial periodicity range (Zone 8, Fig. 4h). Fast-DO cycles, on the contrary, do not appear to receive much energy from astronomical periodicities (Zone 7, Fig. 4g), but are "fuelled" by a combination of centennial climate cycles and secondary interactions with other fast-DO periodicities (Zones 6–9, Fig. 4f–i).

4. Potential cryospheric and climatic energy-transfer mechanisms

By statistically reanalysing the NGRIP $\delta^{18}O_{ice}$ record, we find clear confirmatory (Petersen et al., 2013;Vettoretti and Peltier, 2018) evidence for two distinct modes (i.e., slow, and fast) of DO variability (Fig. 1c and Fig. 3b). Furthermore, based on our advanced bispectral analyses (Figs. 2, 3b, and 4), we show that separate fuelling pathways underpin these two modes of DO cyclicity. If these interpretations are correct, then slow-DO cycles constitute a nonlinear response primarily to

https://doi.org/10.5194/cp-2023-6
Preprint. Discussion started: 24 February 2023


Climate of the Past Discussions

astronomical climate forcing (Wara et al., 2000;Hagelberg et al., 1994;Sun et al., 2021;Zhang et al., 2021), which in combination with secondary energy-redistributing mechanisms among slow-DO periodicities results in T_{air} cyclicity over Greenland in the 12.5 to 2.5 kyr bandwidth. We speculate that these mechanisms were predominantly linked to the Northern Hemisphere cryosphere (Vettoretti and Peltier, 2018), for example the regeneration time, or waiting time (Alley et al., 2001), of grounded ice in the Hudson Bay following catastrophic collapses (Boers et al., 2018). Such a mechanism would have affected sea-ice cover and regional T_{air}, most probably also over Greenland. Furthermore, the relatively long time periods needed for ice sheets to respond, are in line with a relatively slow mode of DO cyclicity.

For fast-DO cycles, the energy redistributing mechanisms are not as straightforward as those for slow-DO cycles. However, our results suggest that many, closely spaced energy exchanges in the frequency domain (see e.g., the rapidly alternating losses and gains in Fig. 3b), may serve as a primary energy source for fast-DO cycles in the 1.5 ± 0.5 kyr bandwidth. Although energy for fast-DO cycles may be collected from many centennial periodicities, mainly in the 0.3 to 0.1 kyr range (Fig. 3b and 4), initially this energy was probably derived from long-term modulations in the solar cycles (Wagner et al., 2001;Peristykh and Damon, 2003), or derived from even shorter-periodic (e.g., decadal) sunspot cycles not captured here. We tentatively support a solar forcing hypothesis for fast-DO cycles, albeit not through a summing of periodicities (Braun et al., 2005), but through nonlinear energy exchanges with shorter periodicities. We speculate that changes in ocean currents and/or tides, due to their destabilizing effects on ice shelfs (Dokken et al., 2013;Griem et al., 2019;Vettoretti and Peltier, 2018), may be the primary driver for the distinct fast-DO mode of variability. Shelf collapse and rapid warming followed by a slower phase of shelf re-expansion, would explain the asymmetric shape of the 1.5 ± 0.5 kyr $\delta^{18}O_{ice}$/air temperature cycles (Schulz et al., 1999).

5 Conclusions

DO cycles, both slow and fast, probably resulted, at least in part, from cryospheric and potentially oceanic energy-redistributing processes (Schulz et al., 2002;Boers et al., 2018;Schulz, 2002;Schulz et al., 1999) that operated on a broad continuum of periodicities and linked dynamic behaviour across time scales. These processes were likely amplified through positive feedbacks of the carbon cycle (Brook et al., 1996;Bauska et al., 2021;Vettoretti et al., 2022). We provide a description of two distinct energy transfer pathways: one from longer astronomical periodicities, and one from shorter centennial periodicities to the millennial periodicities that mark DO cycles. These findings contrast with previous studies that favour more singular mechanisms to explain both slow and fast DO cyclicity (e.g., (Lohmann and Svensson, 2022;Petersen et al., 2013;Vettoretti et al., 2022)). The bispectrum can only assess net energy exchanges among periodic components of a time series, and hence, we cannot rule out non-periodic, non-energy redistributing forcing factors, such as volcanism (Crick et al., 2021;Paine et al., 2021;Lohmann and Svensson, 2022;Lin et al., 2022), asteroid impacts (van Hoesel et al., 2014), and/or noise induced or other "stochastic events" (Alley et al., 2001;Braun et al., 2009;Lohmann et al., 2020;Vettoretti et al.,

https://doi.org/10.5194/cp-2023-6
Preprint. Discussion started: 24 February 2023


Climate of the Past Discussions

2022). However, our study stresses the importance of considering nonlinear, but deterministic, energy-redistributing mechanisms within the climate-cryosphere system to explain periodic signals on time scales without primary periodic energy-sources.

Appendices

Appendix A: NGRIP age model. The NGRIP record is composed of two bore holes that are spliced together. These cores recovered snow and ice layers with annual resolution. To generate a high-fidelity time series 20 layers were averaged, yielding a highly reproducible and largely noise-free $\delta^{18}O_{ice}$ chronology. The ice-water $\delta^{18}O$ record constitutes an T_{air} proxy record of the past 123 kyr that captures astronomical, millennial, and centennial climate variability in exquisite detail (Andersen et al., 2004;Kindler et al., 2014) (Fig. 1). The "GICC05modelext" age model (Vinther et al., 2006;Rasmussen et al., 2006;Andersen et al., 2006;Svensson et al., 2008;Wolff et al., 2010) used here, was constructed using a combination of annual ice layer counting and an ice flow model. We note that the relatively small age model differences (up to ~0.5 kyr) compared to the older "ss09sea" age model (Andersen et al., 2004) do not affect the outcome of bispectral analyses, because bispectra assess cycle geometry in the frequency domain, which allows for modest changes in the time domain (Liebrand and de Bakker, 2019).

Appendix B: Statistical analyses. The wavelet analysis of the NGRIP $\delta^{18}O_{ice}$ record transforms the time series into the time-periodicity domain using a Morlet wavelet (Fig. 1c). Prior to the wavelet analysis only, we applied a Gaussian notch filter (f = 0 kyr^{-1}, bandwidth = 0.05 kyr^{-1}) to the NGRIP $\delta^{18}O_{ice}$ record (50-year sample spacing) to slightly enhance the power of the millennial periodicities with respect to the astronomical periodicities.

In this study, we use the same bispectral methods as described in Liebrand and de Bakker (2019). In short: the bispectrum is defined by Eq. (1):

$$B_{f_1, f_2} = E[C_{f_1} C_{f_2} C^*_{f_1+f_2}], \quad (1)$$

where $E[\ldots]$ is the ensemble average of the triple product of complex Fourier coefficients C at the difference frequencies f_1, f_2, and their sum f_3 (i.e., $= f_1 + f_2$), and the asterisk indicates complex conjugation (Hasselmann et al., 1963). To extract the total gain or loss in energy per climate cycle over the 123 kyr span of the NGRIP $\delta^{18}O_{ice}$ record, and hence, to obtain conservative net energy transfers per frequency (defined by the nonlinear source term S_{nl}), we integrate over the imaginary part of the bispectrum and multiply it with a coupling coefficient. Similar to Liebrand and de Bakker (2019), we make minimum assumptions and use a coupling coefficient that only corrects for frequency $W_{(f_1,f_2)} = (f_1 + f_2)$, which is also part of the Boussinesq scaling used for ocean waves (Herbers and Burton, 1997;Herbers et al., 2000). The correction for frequency ($W_{(f_1,f_2)}$) ensures energy conservation during triad interactions (see Supp. Fig. S3) and permits qualitative

https://doi.org/10.5194/cp-2023-6
Preprint. Discussion started: 24 February 2023


Climate of the Past Discussions

interpretations of conservative net energy exchanges across the spectrum (see Fig. 3b and Fig. 4). We express the integral of S_{nl} in terms of an integration, or summation, over the positive quadrant of the bispectrum alone, or equivalently in sum and difference interactions following Eq. (2):

$$S_{nl,f} = S_{nl,f^+} + S_{nl,f^-}, \quad (2).$$

The difference contributions are expressed by Eq. (3):

$$S_{nl^-} = -2\sum_{f\in F^-} W_{f+f',-f'}\, I\{B_{f,f'}\}. \quad (3)$$

and are obtained by integrating along vertical and horizontal lines, perpendicular to the *x* and *y*-axes, respectively (Fig. 2, Supp. Fig. S2). The sum contributions are expressed by Eq. (4):

$$S_{nl^+} = \sum_{f\in F^+} W_{f',f-f'}\, I\{B_{f',f-f'}\}, \quad (4)$$

and are obtained by integrating diagonally over the bispectrum (Fig. 2, Supp. Fig. S2). Integration can be performed including all frequencies, i.e., a total integration over the entire imaginary part of the bispectrum (Fig. 3b), or over specific zones only, in case subsets of interactions need to be further examined (Fig. 4, Supp. Table S1) (de Bakker et al., 2015;de Bakker et al., 2016).

The imaginary part of the bispectrum, the total, and the zonal integrations, constitute an average of the past 123 ka. Prior to bispectral analysis, the raw NGRIP $\delta^{18}O_{ice}$ record (20-year sample spacing) was linearly detrended and multiplied by a Hamming window function. We subsequently used an energy correction factor that corrects for the Hamming tapering. Previous statistical analyses (Liebrand and de Bakker, 2019) have shown that this approach considerably clarifies the bispectral results. However, we note that resulting from the tapering, nonlinear triad interactions in the central part of the time-series are relatively over-represented, whereas those on either end of the record (i.e., the Eemian, Bølling–Allerød/Younger Dryas, and Holocene) are relatively underrepresented in the bispectral analysis.

Following studies on ocean waves (Herbers et al., 2000;de Bakker et al., 2015), we focus the interpretation on the imaginary part of the bispectrum (Figs. 2, 3b, and 4), which is related to cycle asymmetry, because most energy transfers are associated with asymmetric cycle shapes/wave forms. Furthermore, we visually observe sawtoothshaped/asymmetric climate cycles in the NGRIP $\delta^{18}O_{ice}$ record, associated with both slow and fast DO cycles. It is key to note that the asymmetry/sawtoothness of DO cycles, analysed here using the imaginary part of the bispectrum, is distinct from their skewness/peakedness (Ditlevsen et al., 2005), which is deconvolved in the real part of the bispectrum, or from excess kurtosis/rectangularity/square-waveness (Hinnov et al., 2002;Ditlevsen et al., 1996), which is deconvolved in the trispectrum. The latter two constitute wholly different nonsinusoidal cycle properties (Hagelberg et al., 1991;King, 1996). Skewed and kurtose cycle geometries are not as straightforwardly associable with energy transfers (Liebrand and de Bakker, 2019;de Bakker et al., 2015;Herbers et al., 2000).

https://doi.org/10.5194/cp-2023-6
Preprint. Discussion started: 24 February 2023


Climate of the Past Discussions

The bispectrum yields nonconservative relative energy transfers that have not yet been corrected for frequency (Liebrand and de Bakker, 2019;de Bakker et al., 2015). Prior to such a scaling, the relative energy transfers at higher frequencies are not as pronounced as those at lower frequencies in the bispectrum (Fig. 2). During the integration of the bispectrum, we scale energy transfers to frequency by assuming a standard coupling coefficient, which is based on the second order Boussinesq theory (Herbers and Burton, 1997;Herbers et al., 2000). This scaling yields conservative net energy transfers for the imaginary part of the bispectrum only (Liebrand and de Bakker, 2019;de Bakker et al., 2015) (Fig. 3, 4, and Supp. Fig. S3). We note, however, that both the nonconservative relative energy transfers of the bispectrum, as well as the conservative net energy transfers of the integration of the bispectrum, are not absolute (Liebrand and de Bakker, 2019). We forego scaling energy transfers to insolation due to the many unknowns in the climate-cryosphere system that link changes in insolation (i.e., in W m^2) to changes in $\delta^{18}O_{ice}$ (i.e., in ‰).

Code availability

The detailed mathematical description of the bispectral analyses used in this study are presented in Appendix B as well as in de Bakker et al., (2015) and Liebrand and de Bakker (2019). Code will be made available on individual request to the corresponding authors.

Data availability

The NGRIP $\delta^{18}O_{ice}$ record can be downloaded here: https://www.iceandclimate.nbi.ku.dk/data/2010-11-19_GICC05modelext_for_NGRIP.xls

Author contributions

D.L. and A.T.M.d.B. designed the study, performed the data analysis, and made the figures. A.T.M.d.B. adjusted the bispectral MATLAB scripts for the purposes of this study. All authors discussed the interpretation of the results and contributed to the writing of the manuscript.

Competing interests

The authors declare no competing interests.

https://doi.org/10.5194/cp-2023-6
Preprint. Discussion started: 24 February 2023

Climate of the Past Discussions

Acknowledgements

This project was funded in part by (*i*) the Deutsche Forschungsgemeinschaft (DFG) through a Cluster of Excellence grant awarded to MARUM, and (*ii*) the Natural Environment Research Council (NERC) through funding awarded to the British Ocean Sediment COre Research Facility (BOSCORF) and (*iii*) through NERC grant #NE/X002519/1 awarded to Dr. Neil C. Mitchell. We thank the NGRIP members and the wider ice-core drilling and science community for making the $\delta^{18}O_{ice}$ data and accompanying age models available. We thank T. H. C. Herbers and B. G. Ruessink for making their original bispectral MATLAB scripts available, which were adapted for this study. We thank A. Yool for help with the three-dimensional visualization of the wavelet analysis.

References

Alley, R. B., Anandakrishnan, S., and Jung, P.: Stochastic resonance in the North Atlantic, Paleoceanography, 16, 190–198, 2001.

Andersen, K. K., Azuma, N., Barnola, J. M., Bigler, M., Biscaye, P., Caillon, N., Chappellaz, J., Clausen, H. B., DahlJensen, D., Fischer, H., Fluckiger, J., Fritzsche, D., Fujii, Y., Goto-Azuma, K., Gronvold, K., Gundestrup, N. S., Hansson, M., Huber, C., Hvidberg, C. S., Johnsen, S. J., Jonsell, U., Jouzel, J., Kipfstuhl, S., Landais, A., Leuenberger, M., Lorrain, R., Masson-Delmotte, V., Miller, H., Motoyama, H., Narita, H., Popp, T., Rasmussen, S. O., Raynaud, D., Rothlisberger, R., Ruth, U., Samyn, D., Schwander, J., Shoji, H., Siggard-Andersen, M. L., Steffensen, J. P., Stocker, T., Sveinbjornsdottir, A. E., Svensson, A., Takata, M., Tison, J. L., Thorsteinsson, T., Watanabe, O., Wilhelms, F., White, J. W. C., and Project, N. G. I. C.: High-resolution record of Northern Hemisphere climate extending into the last interglacial period, Nature, 431, 147–151, 2004.

Andersen, K. K., Svensson, A., Johnsen, S. J., Rasmussen, S. O., Bigler, M., Rothlisberger, R., Ruth, U., Siggaard-Andersen, M. L., Steffensen, J. P., Dahl-Jensen, D., Vinther, B. M., and Clausen, H. B.: The Greenland Ice Core Chronology 2005, 15-42 ka. Part 1: constructing the time scale, Quaternary Sci Rev, 25, 3246–3257, 2006.

Bauska, T. K., Marcott, S. A., and Brook, E. J.: Abrupt changes in the global carbon cycle during the last glacial period, Nat Geosci, 14, 91–96, 2021.

Boers, N., Ghil, M., and Rousseau, D.-D.: Ocean circulation, ice shelf, and sea ice interactions explain Dansgaard–Oeschger cycles, P Natl Acad Sci USA, 115, 2018.

Braun, H., Christl, M., Rahmstorf, S., Ganopolski, A., Mangini, A., Kubatzki, C., Roth, K., and Kromer, B.: Possible solar origin of the 1,470-year glacial climate cycle demonstrated in a coupled model, Nature, 438, 208–211, 2005.

Braun, H., Ditlevsen, P., and Kurths, J.: New measures of multimodality for the detection of a ghost stochastic resonance, Chaos, 19, 1–12, 2009.

Brook, E. J., Sowers, T., and Orchardo, J.: Rapid variations in atmospheric methane concentration during the past 110,000 Years, Science, 273, 1087–1091, 1996.

https://doi.org/10.5194/cp-2023-6
Preprint. Discussion started: 24 February 2023

Corrick, E. C., Drysdale, R. N., Hellstrom, J. C., Capron, E., Rasmussen, S. O., Zhang, X., Fleitmann, D., Couchoud, I., and Wolff, E.: Synchronous timing of abrupt climate changes during the last glacial period, Science, 369, 963–969, 2020.

Crick, L., Burke, A., Hutchison, W., Kohno, M., Moore, K. A., Savarino, J., Doyle, E. A., Mahony, S., Kipfstuhl, S., Rae, J. W. B., Steele, R. C. J., Sparks, R. S. J., and Wolff, E.: New insights into the 74 ka Toba eruption from sulfur isotopes of polar ice cores, Clim Past, 17, 2119–2137, 2021.

Dansgaard, W., Johnsen, S. J., Clausen, H. B., Dahl-Jensen, D., Gundestrup, N., Hammer, C. U., and Oeschger, H.: North Atlantic climatic oscillations revealed by deep Greenland ice cores, in: Climate processes and climate sensitivity, edited by: Hansen, J. E., and Takahashi, T., American Geophysical Union, Washington D.C. , 288–298, 1984.

Dansgaard, W., Johnsen, S. J., Clausen, H. B., Dahljensen, D., Gundestrup, N. S., Hammer, C. U., Hvidberg, C. S., Steffensen, J. P., Sveinbjornsdottir, A. E., Jouzel, J., and Bond, G.: Evidence for general instability of past climate from a 250-Kyr ice-core record, Nature, 364, 218–220, 1993.

de Bakker, A. T. M., Herbers, T. H. C., Smit, P. B., Tissier, M. F. S., and Ruessink, B. G.: Nonlinear infragravity-wave interactions on a gently sloping laboratory beach, Journal of Physical Oceanography, 45, 589–605, 2015.

de Bakker, A. T. M., Tissier, M. F. S., and Ruessink, B. G.: Beach steepness effects on nonlinear infragravity-wave interactions: A numerical study, J Geophys Res-Oceans, 121, 554–570, 2016.

Ditlevsen, P. D., Svensmark, H., and Johnsen, S.: Contrasting atmospheric and climate dynamics of the last-glacial and Holocene periods, Nature, 379, 810-812, 1996.

Ditlevsen, P. D., Kristensen, M. S., and Andersen, K. K.: The recurrence time of Dansgaard-Oeschger events and limits on the possible periodic component, J Climate, 18, 2594–2603, 2005.

Ditlevsen, P. D., Andersen, K. K., and Svensson, A.: The DO-climate events are probably noise induced: statistical investigation of the claimed 1470 years cycle, Clim Past, 3, 129–134, 2007.

Dokken, T. M., Nisancioglu, K. H., Li, C., Battisti, D. S., and Kissel, C.: Dansgaard-Oeschger cycles: Interactions between ocean and sea ice intrinsic to the Nordic seas, Paleoceanography, 28, 491–502, 10.1002/palo.20042, 2013.

Gottwald, G. A.: A model for Dansgaard–Oeschger events and millennial-scale abrupt climate change without external forcing, Clim Dynam, 56, 227–243, 2021.

Griem, L., Voelker, A. H. L., Berben, S. M. P., Dokken, T. M., and Jansen, E.: Insolation and Glacial Meltwater Influence on Sea-Ice and Circulation Variability in the Northeastern Labrador Sea During the Last Glacial Period, Paleoceanogr Paleocl, 2019.

Hagelberg, T., Pisias, N., and Elgar, S.: Linear and nonlinear couplings between orbital forcing and the marine $\delta^{18}O$ record during the late Neogene, Paleoceanography, 6, 729–746, 1991.

https://doi.org/10.5194/cp-2023-6
Preprint. Discussion started: 24 February 2023

Hagelberg, T. K., Bond, G., and deMenocal, P.: Milankovitch Band Forcing of Sub-Milankovitch Climate Variability during the Pleistocene, Paleoceanography, 9, 545–558, 1994.

Hasselmann, K., Munk, W., and MacDonald, G.: Bispectra of ocean waves, in: Proceedings of the Symposium on Time Series Analysis, edited by: Rosenblatt, M., John Wiley, 125–139, 1963.

Hays, J. D., Imbrie, J., and Shackleton, N. J.: Variations in the Earth's orbit - Pacemaker of the ice ages, Science, 194, 1121–1132, 1976.

Herbers, T. H. C., and Burton, M. C.: Nonlinear shoaling of directionally spread waves on a beach, J Geophys Res-Oceans, 102, 21101–21114, 1997.

Herbers, T. H. C., Russnogle, N. R., and Elgar, S.: Spectral energy balance of breaking waves within the surf zone, Journal of Physical Oceanography, 30, 2723–2737, 2000.

Hinnov, L. A., Schulz, M., and Yiou, P.: Interhemispheric space-time attributes of the Dansgaard-Oeschger oscillations between 100 and 0 ka, Quaternary Sci Rev, 21, 1213–1228, 2002.

Huybers, P., and Curry, W.: Links between annual, Milankovitch and continuum temperature variability, Nature, 441, 329–332, 2006.

Kelsey, A. M.: Abrupt climate change and millennial-scale cycles: an astronomical mechanism, Climate of the Past Discussions, 2022.

Kindler, P., Guillevic, M., Baumgartner, M., Schwander, J., Landais, A., and Leuenberger, M.: Temperature reconstruction from 10 to 120 kyr b2k from the NGRIP ice core, Clim Past, 10, 887–902, 2014.

King, T.: Quantifying nonlinearity and geometry in time series of climate, Quaternary Sci Rev, 15, 247–266, 1996.

Kleppin, H., Jochum, M., Otto-Bliesner, B., Shields, C. A., and Yeager, S.: Stochastic Atmospheric Forcing as a Cause of Greenland Climate Transitions, J Climate, 28, 7741–7763, 10.1175/Jcli-D-14-00728.1, 2015.

Laskar, J., Robutel, P., Joutel, F., Gastineau, M., Correia, A. C. M., and Levrard, B.: A long-term numerical solution for the insolation quantities of the Earth, Astronomy and Astrophysics, 428, 261–285, 2004.

Liebrand, D., and de Bakker, A. T. M.: Bispectra of climate cycles show how ice ages are fuelled, Clim Past, 15, 1959–1983, 2019.

Lin, J., Svensson, A., Hvidberg, C. S., Lohmann, J., Kristiansen, S., Dahl-Jensen, D., Steffensen, J. P., Rasmussen, S. O., Cook, E., Kjær, H. A., Vinther, B. M., Fischer, H., Stocker, T., Sigl, M., Bigler, M., Severi, M., Traversi, R., and Mulvaney, R.: Magnitude, frequency and climate forcing of global volcanism during the last glacial period as seen in Greenland and Antarctic ice cores (60–9 ka), Clim Past, 18, 485–506, 2022.

https://doi.org/10.5194/cp-2023-6
Preprint. Discussion started: 24 February 2023

Lohmann, G., Butzin, M., Eissner, N., Shi, X., and Stepanek, C.: Abrupt climate and weather changes across time scales, Paleoceanogr Paleocl, 35, 2020.

Lohmann, J., and Svensson, A.: Ice core evidence for major volcanic eruptions at the onset of Dansgaard-Oeschger warming events, Climate of the Past Discussions, 2022.

Loulergue, L., Schilt, A., Spahni, R., Masson-Delmotte, V., Blunier, T., Lemieux, B., Barnola, J.-M., Raynaud, D., Stocker, T. F., and Chappellaz, J.: Orbital and millennial-scale features of atmospheric CH_4 over the past 800,000 years, Nature, 453, 383–386, 2008.

Matyasovszky, I.: Trends, time-varying and nonlinear time series models for NGRIP and VOSTOK paleoclimate data, Theoretical and applied climatology, 101, 433-443, 2010.

Menviel, L. C., Skinner, L. C., Tarasov, L., and Tzedakis, P. C.: An ice-climate oscillatory framework for Dansgaard–Oeschger cycles, Nature Reviews | Earth & Environment, 1, 677–693, 2020.

Mitsui, T., Lenoir, G., and Crucifix, M.: Is the glacial climate scale invariant?, Dynamics and Statistics of the Climate System, 3, 2019.

Paine, A. R., Wadsworth, F. B., and Baldini, J. U. L.: Supereruption doublet at a climate transition, Communications Earth & Environment, 2, 2021.

Pelletier, J. D.: The power spectral density of atmospheric temperature from time scales of 10^{-2} to 10^{6} yr, Earth Planet Sc Lett, 158, 157–164, 1998.

Peristykh, A. N., and Damon, P. E.: Persistence of the Gleissberg 88-year solar cycle over the last ~12,000 years: Evidence from cosmogenic isotopes, Journal of Geophysical Research, 108, 2003.

Pestiaux, P., Van der Mersch, I., Berger, A., and Duplessy, J. C.: Paleoclimatic variability at frequencies ranging from 1 cycle per 10 000 years to 1 cycle per 1000 years: evidence for nonlinear behaviour of the climate system, Climatic Change, 12, 9–37, 1988.

Petersen, S. V., Schrag, D. P., and Clark, P. U.: A new mechanism for Dansgaard-Oeschger cycles, Paleoceanography, 28, 24–30, 2013.

Rasmussen, S. O., Andersen, K. K., Svensson, A. M., Steffensen, J. P., Vinther, B. M., Clausen, H. B., Siggaard-Andersen, M.-L., Johnsen, S. J., Larsen, L. B., Dahl-Jensen, D., Bigler, M., Röthlisberger, R., Fischer, H., Goto-Azuma, K., Hansen, M. E., and Ruth, U.: A new Greenland ice core chronology for the last glacial termination, Journal of Geophysical Research, 111, 1–16, 2006.

Rasmussen, S. O., Bigler, M., Blockley, S. P., Blunier, T., Buchardt, S. L., Clausen, H. B., Cvijanovic, I., Dahl-Jensen, D., Johnsen, S. J., Fischer, H., Gkinis, V., Guillevic, M., Hoek, W. Z., Lowe, J. J., Pedro, J. B., Popp, T., Seierstad, I. K., Steffensen, J. P., Svensson, A. M., Vallelonga, P., Vinther, B. M., Walker, M. J. C., Wheatley, J. J., and Winstrup, M.: A

https://doi.org/10.5194/cp-2023-6
Preprint. Discussion started: 24 February 2023

stratigraphic framework for abrupt climatic changes during the Last Glacial period based on three synchronized Greenland ice-core records: refining and extending the INTIMATE event stratigraphy, Quaternary Sci Rev, 106, 14–28, 2014.

Riechers, K., Mitsui, T., Boers, N., and Ghil, M.: Orbital insolation variations, intrinsic climate variability, and Quaternary glaciations, Clim Past, 18, 869–893, 2022.

Rousseau, D.-D., Bagniewski, W., and Ghil, M.: Abrupt climate changes and the astronomical theory: are they related?, Clim Past, 18, 249–271, 2022.

Scafetta, N., Milani, F., Bianchini, A., and Ortolani, S.: On the astronomical origin of the Hallstatt oscillation found in radiocarbon and climate records throughout the Holocene, Earth-Science Reviews, 162, 24–43, 2016.

Schulz, M., Berger, W. H., Sarnthein, M., and Grootes, P. M.: Amplitude variations of 1470-year climate oscillations during the last 100,000 years linked to fluctuations of continental ice mass, Geophys Res Lett, 26, 3385–3388, 1999.

Schulz, M.: On the 1470-year pacing of Dansgaard-Oeschger warm events, Paleoceanography, 17, 2002.

Schulz, M., Paul, A., and Timmermann, A.: Relaxation oscillators in concert: A framework for climate change at millennial timescales during the late Pleistocene, Geophys Res Lett, 29, 2002.

Shackleton, N. J., Hall, M. A., and Vincent, E.: Phase relationships between millennial-scale events 64,000-24,000 years ago, Paleoceanography, 15, 565–569, 2000.

Stuiver, M., and Braziunas, T. F.: Sun, ocean, climate and atmospheric $^{14}CO_2$: an evaluation of causal and spectral relationships, The Holocene, 3, 289–305, 1993.

Sun, Y., McManus, J. F., Clemens, S. C., Zhang, X., Vogel, H., Hodell, D. A., Guo, F., Wang, T., Liu, X., and An, Z.: Persistent orbital influence on millennial climate variability through the Pleistocene, Nat Geosci, 14, 812–818, 2021.

Svensson, A., Andersen, K. K., Bigler, M., Clausen, H. B., Dahl-Jensen, D., Davies, S. M., Johnsen, S. J., Muscheler, R., Parrenin, F., Rasmussen, S. O., Röthlisberger, R., Seierstad, I., Steffensen, J. P., and Vinther, B. M.: A 60 000 year Greenland stratigraphic ice core chronology, Clim Past, 4, 47–57, 2008.

van Hoesel, A., Hoek, W. Z., Pennock, G. M., and Drury, M. R.: The Younger Dryas impact hypothesis: a critical review, Quaternary Sci Rev, 83, 95–114, 2014.

Vettoretti, G., and Peltier, W. R.: Fast Physics and Slow Physics in the Nonlinear Dansgaard–Oeschger Relaxation Oscillation, J Climate, 31, 3423–3449, 2018.

Vettoretti, G., Ditlevsen, P., Jochum, M., and Rasmussen, S. O.: Atmospheric CO_2 control of spontaneous millennial-scale ice age climate oscillations, Nat Geosci, 15, 300–306, 2022.

https://doi.org/10.5194/cp-2023-6
Preprint. Discussion started: 24 February 2023

Vinther, B. M., Clausen, H. B., Johnsen, S. J., Rasmussen, S. O., Andersen, K. K., Buchardt, S. L., Dahl-Jensen, D., Seierstad, I. K., Siggaard-Andersen, M.-L., Steffensen, J. P., Svensson, A., Olsen, J., and Heinemeier, J.: A synchronized dating of three Greenland ice cores throughout the Holocene, Journal of Geophysical Research, 111, 1–11, 2006.

Wagner, G., Beer, J., Masarik, J., and Muscheler, R.: Presence of the solar de Vries cycle (205 years) during the last ice age, Geophys Res Lett, 28, 303-306, 2001.

Wara, M. W., Ravelo, A. C., and Revenaugh, J. S.: The pacemaker always rings twice, Paleoceanography, 15, 616–624, 2000.

Wolff, E. W., Chappellaz, J., Blunier, T., Rasmussen, S. O., and Svensson, A.: Millennial-scale variability during the last glacial: The ice core record, Quaternary Sci Rev, 29, 2828–2838, 2010.

Zhang, X., Barker, S., Knorr, G., Lohmann, G., Drysdale, R., Sun, Y., Hodell, D., and Chen, F.: Direct astronomical influence on abrupt climate variability, Nat Geosci, 14, 819–826, 2021.

https://doi.org/10.5194/cp-2023-6
Preprint. Discussion started: 24 February 2023

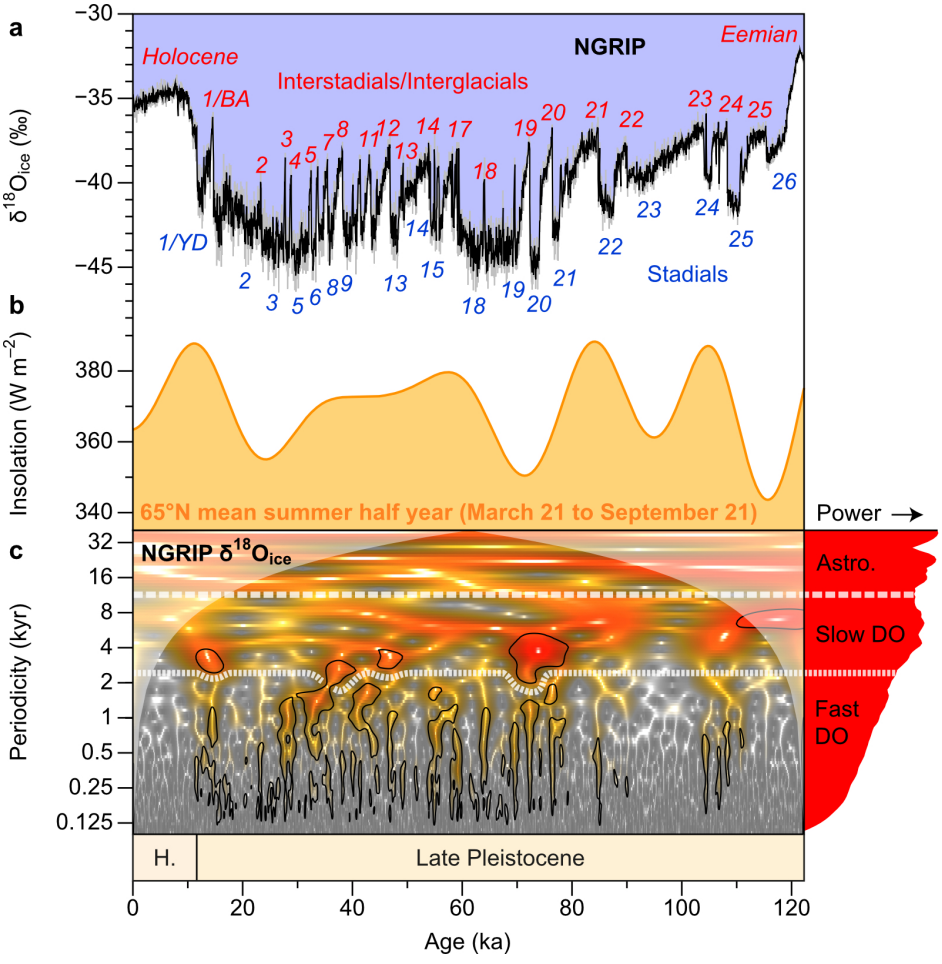

445 **Figure 1: The NGRIP $\delta^{18}O_{ice}$ record versus summer insolation at 65° N.** (**a**) The NGRIP $\delta^{18}O_{ice}$ record on the "GICC05modelext" age model (Vinther et al., 2006;Rasmussen et al., 2006;Andersen et al., 2006;Svensson et al., 2008;Wolff et al., 2010) versus (**b**) mean summer half year insolation at 65° N (March 21 to September 21) for the past 123 ka (Laskar et al., 2004). In panel (**a**): grey line represents the NGRIP $\delta^{18}O_{ice}$ record with 20-year sample spacing, used for bispectral analyses (Fig. 2–4). Black line represents the NGRIP $\delta^{18}O_{ice}$ record with a 50-year sample spacing, used for the
450 wavelet analysis (panel **c**). (**c**) Wavelet analysis of the Gaussian filtered NGRIP $\delta^{18}O_{ice}$ record (see Appendix B). Black contours represent the 95% significance level with respect to a red noise model. The colours of the wavelet indicate amplitude (white/grey = low amplitude, yellow/orange/red = high amplitude). We note that colour/amplitude does not equate to statistical significance with respect to the red noise model. An average of the entire wavelet spectrum is shown on the right-hand side in red. The two white dashed lines indicate the spectral gaps between astronomical and slow-DO periodicities
455 (broad dashes), and between slow-DO and fast-DO periodicities (narrow dashes). "H" stands for Holocene, "BA" stands for Bølling–Allerød, and "YD" stands for Younger Dryas. The latter two together correspond to DO Cycle-1.

https://doi.org/10.5194/cp-2023-6
Preprint. Discussion started: 24 February 2023

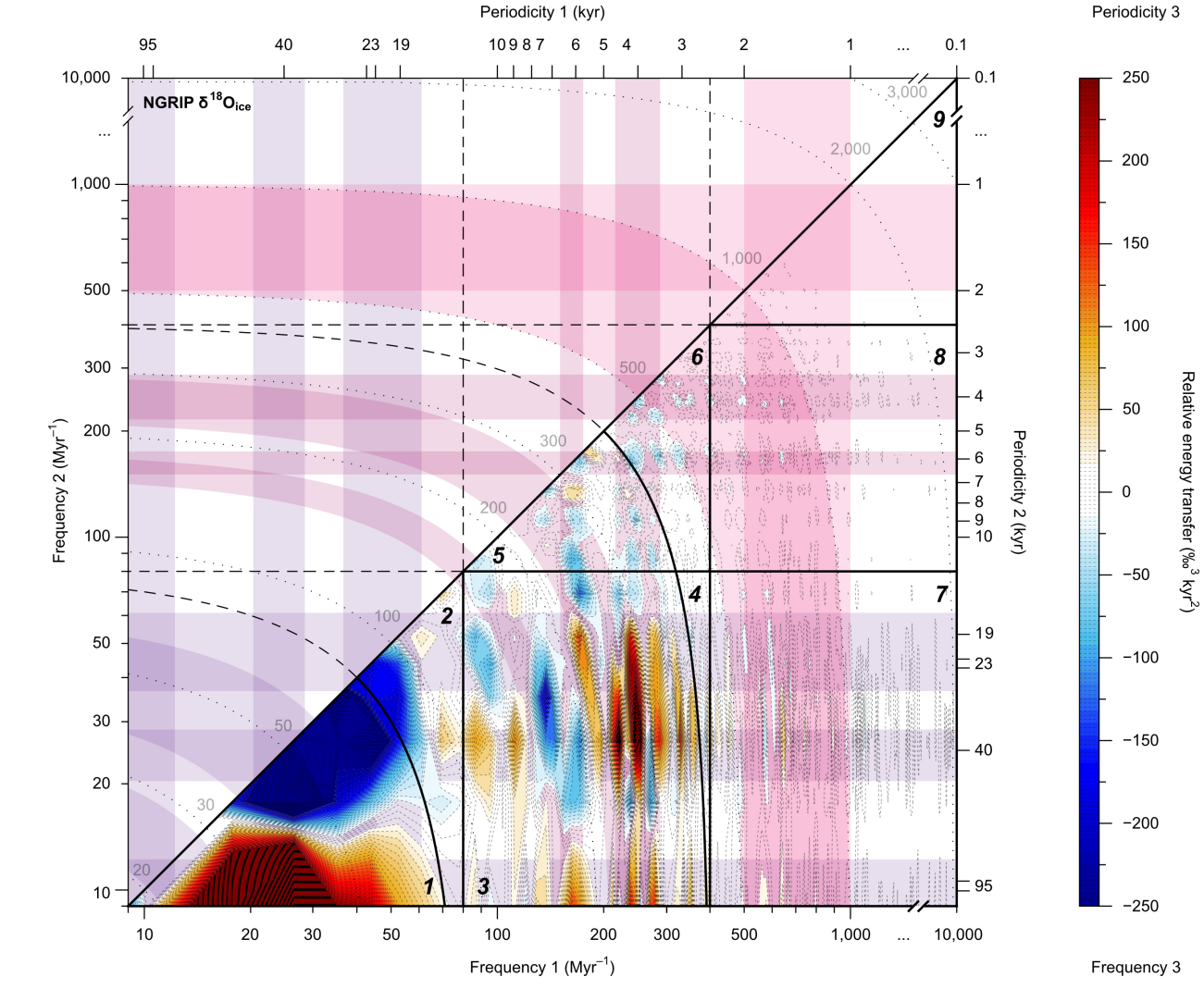

Figure 2: Bispectrum of the NGRIP $\delta^{18}O_{ice}$ record. The imaginary part of the bispectrum of the NGRIP $\delta^{18}O_{ice}$ record depicts energy exchanges among three frequencies. Energy can only be transferred if both frequencies- (f) and phases- (φ) are coupled: $f_1 + f_2 = f_3$ and $\varphi_1 + \varphi_2 = \varphi_3$. The x-axis shows difference-frequency f_1, the y-axis depicts difference-frequency f_2, the colour bar corresponds to sum-frequency f_3 (i.e., $f_1 + f_2$). Two outcomes exist for energy exchanges: either f_3 gains energy and f_1 and f_2 lose energy, which is shown in orange and red colours, or f_3 loses energy and f_1 and f_2 gain energy, which is shown in blue colours. Purple, plum, and pink coloured bands mark the main periodicities for astronomical, slow-, and fast-DO cycles, respectively. Vertical and horizontal coloured-bands mark f_1 and f_2, respectively. Diagonal bands (curved on the log-log scale) mark f_3. Thick solid black lines mark our selected zone boundaries between astronomical, slow-, and fast-DO periodicities. See Supp. Fig. S2 for a linear-linear scale version of this figure. For a more detailed explanation of bispectral analysis we refer to Appendix B and Liebrand and de Bakker (2019).

https://doi.org/10.5194/cp-2023-6
Preprint. Discussion started: 24 February 2023

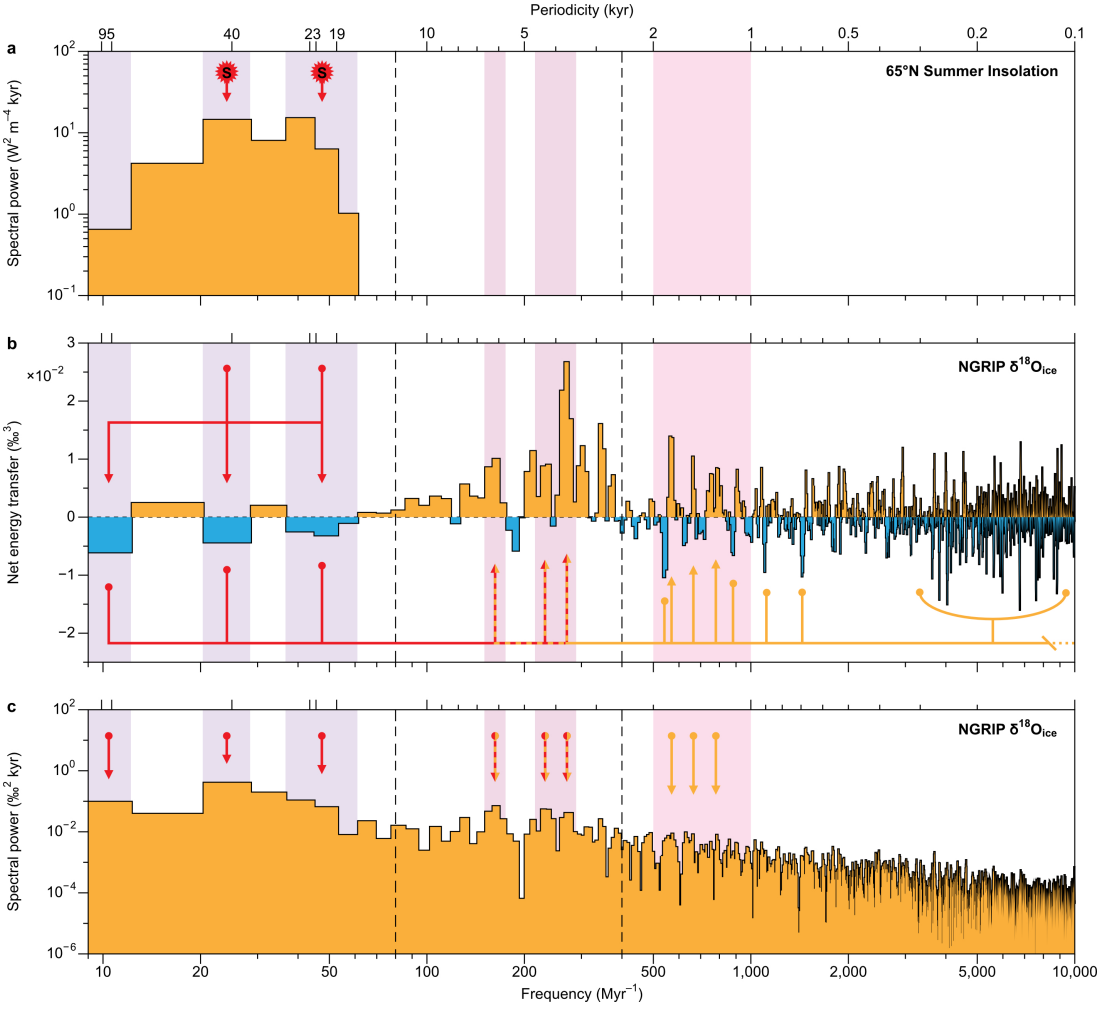

Figure 3: Linking DO cycles to energy sources. Comparison of (**a**) power spectrum of mean summer half year insolation record at 65ºN (March 21 to September 21), to (**b**) total integration of the bispectrum of the NGRIP $\delta^{18}O_{ice}$ record, and (**c**) the power spectrum of the NGRIP $\delta^{18}O_{ice}$ record. Orange indicates spectral power (panel **a** and **c**), or net energy gains (panel **b**), and blue indicates net energy losses (panel **b**). Red and orange arrows indicate the two main energy transfer pathways across the spectral continuum to slow- and fast-DO cycles. These interpretative arrows are derived from both the total (this figure) and the zonal integration (see also Fig. 4). Dashed vertical black lines mark the zone boundaries between astronomical periodicities (purple), slow- (plum), and fast-DO (pink) periodicities. "S" stands for sun/solar forcing, indicating at which frequencies summer insolation provides energy. No 123 kyr long record of sunspot cycles exist, which is why we do not show a spectrum of this energy source here. Furthermore, the highest amplitude spectral power of the solar cycle over the past 123 kyr is expected to fall at around the annual and ~11-year periodicities. These cycles are not resolved in the NGRIP $\delta^{18}O_{ice}$ record, which is marked by a 20-year sample spacing.

https://doi.org/10.5194/cp-2023-6
Preprint. Discussion started: 24 February 2023

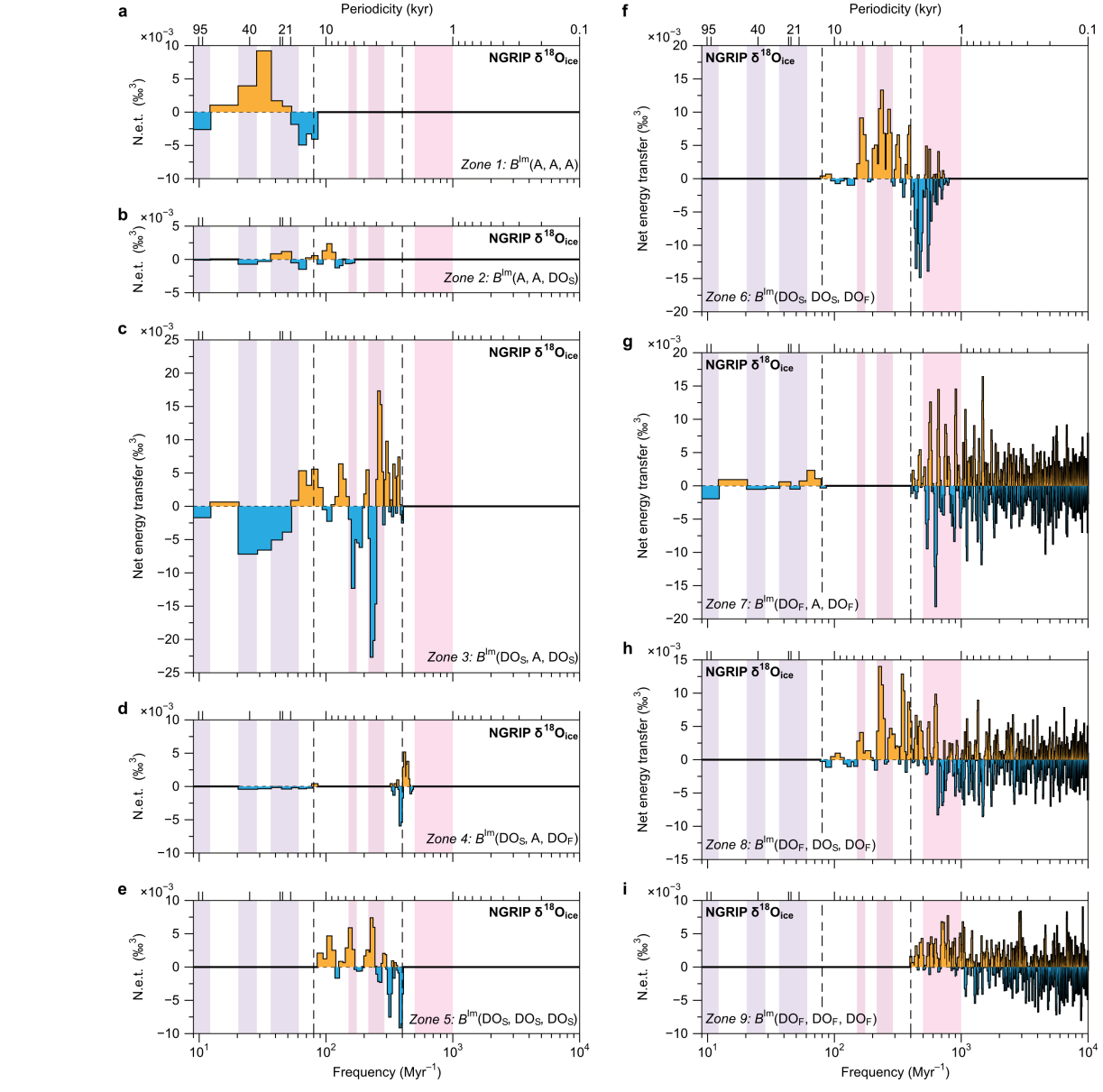

Figure 4: Zonal integrations of the bispectrum. Integrations of (**a**) Zone 1: B^{Im}(A, A, A), (**b**) Zone 2: B^{Im}(A, A, DO_S), (**c**) Zone 3: B^{Im}(DO_S, A, DO_S), (**d**) Zone 4: B^{Im}(DO_S, A, DO_F), (**e**) Zone 5: B^{Im}(DO_S, DO_S, DO_S), (**f**) Zone 6: B^{Im}(DO_S, DO_S, DO_F), (**g**) Zone 7: B^{Im}(DO_F, A, DO_F), (**h**) Zone 8: B^{Im}(DO_F, DO_S, DO_F), and (**i**) Zone 9: B^{Im}(DO_F, DO_F, DO_F). "B^{Im}" stands for the imaginary part of the bispectrum. "A" stands for astronomical periodicities, "DO_S" stands for slow-DO periodicities, "DO_F" stands for fast-DO periodicities. Orange indicates net energy gains, blue net energy losses. Dashed vertical black lines mark the zone boundaries between the main periodicity bandwidths, with the main astronomical periodicities highlighted in purple, slow-DO periodicities in plum, and fast-DO periodicities in pink.